GSA Data Repository 2019376

Dobbs, S.C., et al., 2019, Are submarine and subaerial drainages morphologically distinct?: Geology, v. 47, https://doi.org/10.1130/G46329.1

APPENDIX 1. DATA ACQUISITION AND MANIPULATION

The GMRT synthesizes a series of terrestrial and submarine elevation datasets including ship-based swath multibeam bathymetry data (e.g., data from NOAA NGDC 3 arc sec Coastal Relief Model, Center for Ocean Mapping, Monterey Bay Aquarium Research Institute), and a series of subaerial datasets (e.g., USGS's National Elevation Dataset, Nasa's ASTER global DEM) (Ryan et al., 2009). For the submarine, the synthesis concatenates elevation data from both gridded multi-resolution digital elevation models and ship-based multibeam sonar data whose native resolution is typically 100 m in the deep sea. While bathymetry data are typically processed at 100-m resolution, maximum resolution varies where better quality data are available given certain areas of greater multibeam coverage and/or where more advanced sonar instrumentation was deployed (Ryan et al., 2009; https://www.gmrt.org/about/index.php). In an attempt to merge these datasets while preserving higher resolution DEMs, the GMRT subsamples these high-resolution datasets and supersamples lower resolution datasets with a cell spacing of 61 m. The GMRT does this via a tile set that contains weighted grid nodes whereby higher resolution data are weighted higher, and replace lower-resolution nodes (Ryan et al., 2009). Submarine canyon locations were selected in regions where multibeam data were available, which biases our selection to the US Atlantic margin, US Pacific margin, European Atlantic margin, and part of the Mediterranean Sea. One location, offshore Nova Scotia, is the only exception in regard to resolution, where five of our submarine canyon selections have only partial multibeam coverage towards the upper reaches of the drainage basins. However, we believe given that the large

majority of the basins contain multibeam coverage that the approximate area measurements necessary to estimate steepness and concavity parameters are still within reason. Moreover, removing these analyses from our t-test samples still produces the same results discussed in the main text. Thus, we opted to report these canyons in our analysis even though they do not have full multibeam coverage as their analyses are likely reasonable and these canyons may be of interest to the readers. High latitude regions were also purposefully not selected to avoid any potential effects of recent ice sheets or glaciation. For terrestrial catchments, we selected a diversity of drainages including detachment-limited bedrock systems in mountainous terrains and alluvial, transport-limited systems in low topographic landscapes to reinforce that concavity measurements do indeed fall within a narrow range of values as demonstrated by others (Whipple and Tucker, 1999 and references therein). We also avoided areas of high elevation that could have been recently subject to glaciation and any regions where active faulting could place the system into disequilibrium. Divides were delineated automatically for the case of subaerial watersheds by preventing closed depressions and tracking flow from outlets draining to the edges of each dataset to the internal divides. However, the upper extremities of submarine canyons do not always abut adjacent submarine canyons, and so manual demarcation of the upper watershed extent is necessary. To do this, we manually mapped the location at which canyon heads intersected the continental shelf, and clipped the bathymetry of each canyon to this extent. Furthermore, where drainage divides are not readily apparent, channel edges were also manually clipped (Figs. S1–S2). Subaerial drainages were sampled at roughly the same size of the average submarine canyon drainage area (ca. 3,000 km^2) to avoid scaling anomalies.

APPENDIX 2. COMPARISON OF SUBMARINE DRAINAGE CLASSIFICATIONS

In addition to comparing submarine drainages to subaerial systems, we considered several classifications of submarine catchments to compare with each other. These categories include connectivity with the continental shelf (i.e., shelf indenting vs. slope bound), sinuosity (i.e., sinuous vs. straight channels), and margin type (i.e., passive vs. active). One postulation is that perhaps straighter, elongate canyons that have not reached onto the shelf could represent a more nascent stage canyon that is less developed than their more sinuous, shelf-indenting counterparts (Farre et al., 1983). These class types are provided in our supplemental table (Table S1). We used a set of unpaired, two tail, unequal variance t-tests to test whether or not these categories are unique from one another. In the case of shelf connectivity, there is no significant difference between concavity measurements ($p = 0.702$). To test if sinuosity may highlight different submarine canyon types, we measured the sinuosity (channel length/down-valley length) of each submarine canyon from our dataset (mean sinuosity index = 1.18; $1\sigma = 0.15$) and then compared concavity distributions of low- and high-sinuosity canyons to one another using a two-tailed, unpaired t-test. We found that, when comparing concavity distributions between low (<1.10) and high (≥ 1.10) sinuosity drainages, there is no statistical distinction between the groups ($p = 0.29$). Furthermore, even when comparing concavity distributions between very low sinuosity (<1.05) and very sinuous (>1.30) canyons, there remains no statistical distinction between the two ($p = 0.33$). Thus, while it may be tempting to categorize submarine canyons based on these distinctions, we were not able to statistically discriminate the two in both the case of shelf connectivity and sinuosity in this dataset. Finally, we tested if there are any significant differences in concavity measurements between passive ($n = 24$) and active margin ($n = 5$) submarine drainages. When comparing combined concavities there is no statistical differentiation from each other ($p = 0.18$). However, when only comparing mainstem concavities

to each other, the resultant p-value is lower (p = 0.025), as the mean concavity of active margin mainstems (0.08) is markedly less than the average passive margin concavity (0.34). This might suggest that active margins may have less concave profiles relative to passive margin mainstems. Since our dataset only contains a few active margin examples, we hesitate to claim this is a true distinction and future work would require further analysis of active margin submarine catchments to discern a conclusive relationship. In general, the lack of distinguishing geomorphic categories in the submarine may highlight that, similar to terrestrial channel networks, submarine drainages may also be restricted to a narrow range of concavities, which are, on balance, smaller than subaerial systems.

Table S1. Description of drainage basins analyzed, results from all analyses, and averaged concavity and steepness values for both subaerial and submarine systems. θ_{ms} = mainstem concavity; θ_{tr} = tributary concavity; $^{ms}k_s$ = mainstem steepness; $^{tr}k_s$ = tributary steepness

Figure S1. Example of workflow for processing submarine canyon networks. Shelf edges were clipped for each submarine drainage. In cases where drainage divides are not apparently, channel margins were also clipped manually. A flow-routing algorithm then calculates mainstem and tributary lengths, areas, and an optimization algorithm calculates best-fit k_s and θ values.

Figure S2. Examples of different submarine drainages that were analyzed. Canyons are named are location information is available in Table S1. The blue line indicates the canyon mainstem, while the red lines are the tributaries.

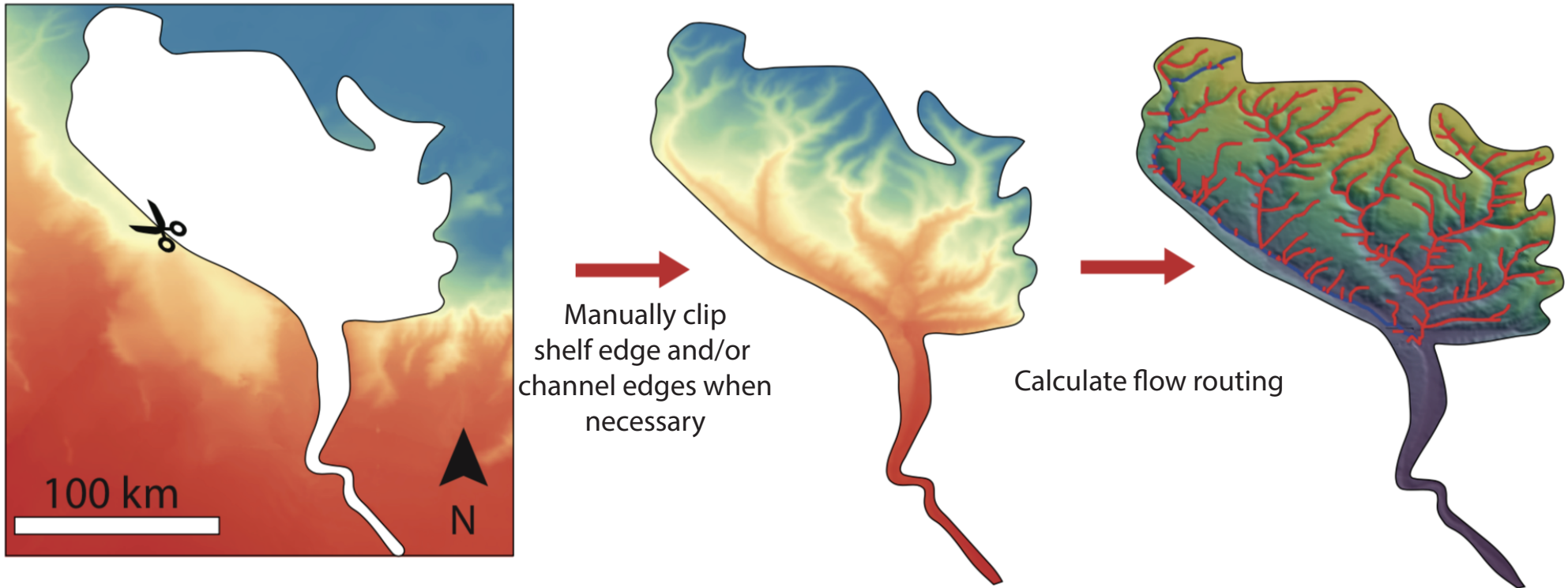

DOBBS FIGURE S1

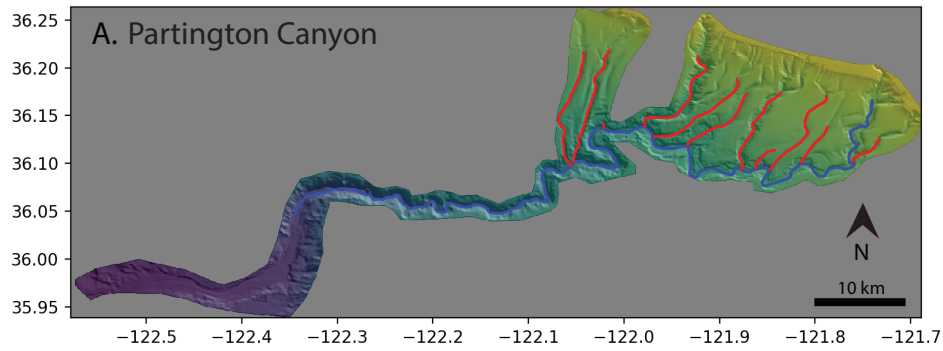

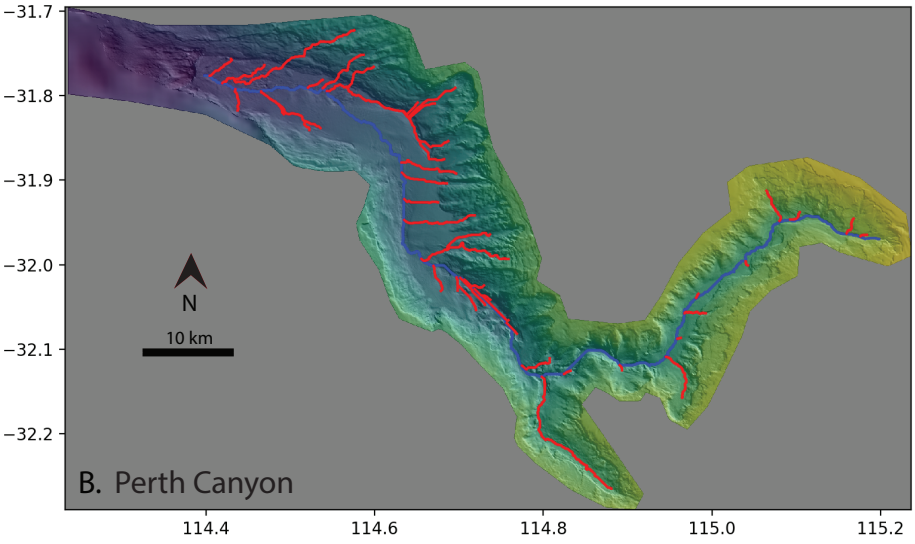

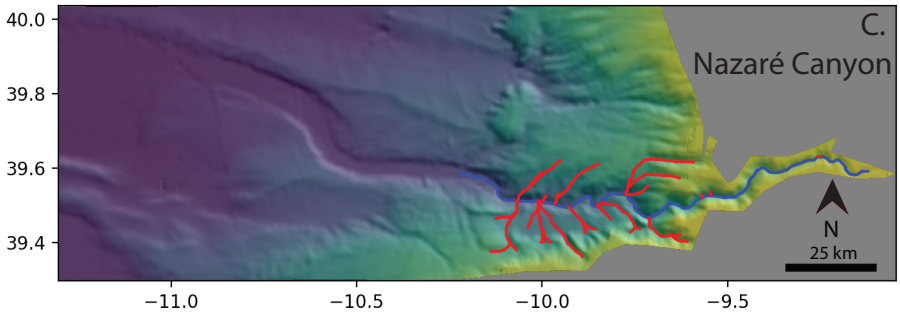

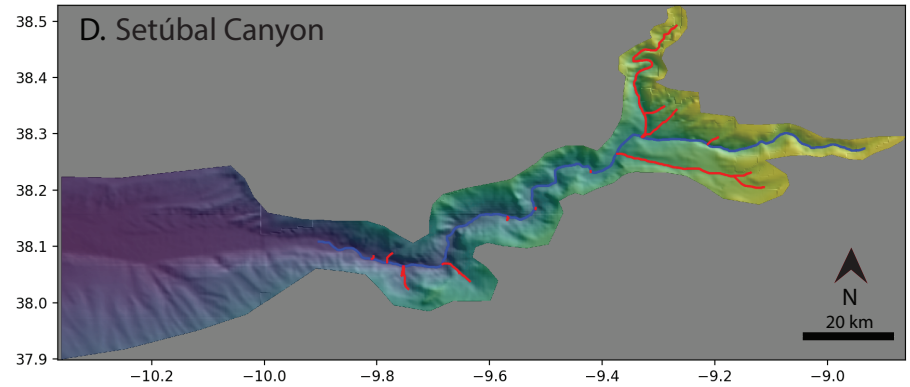

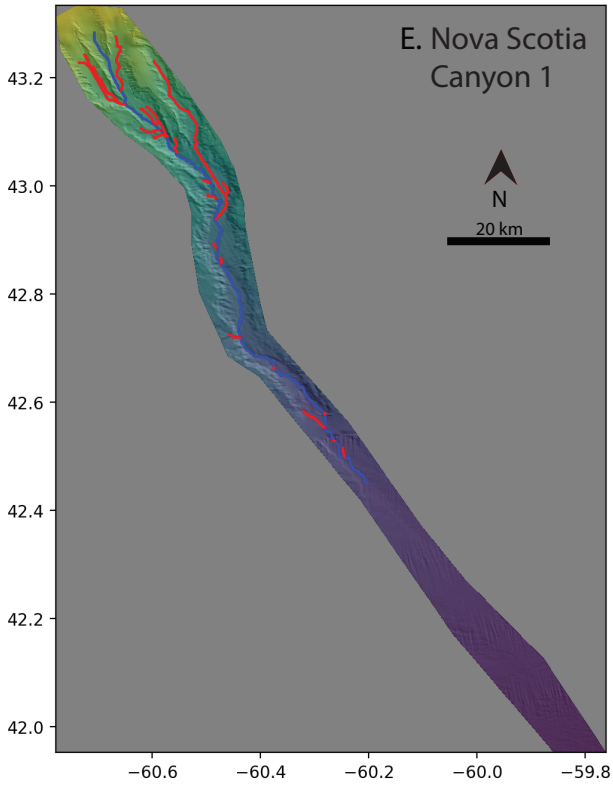

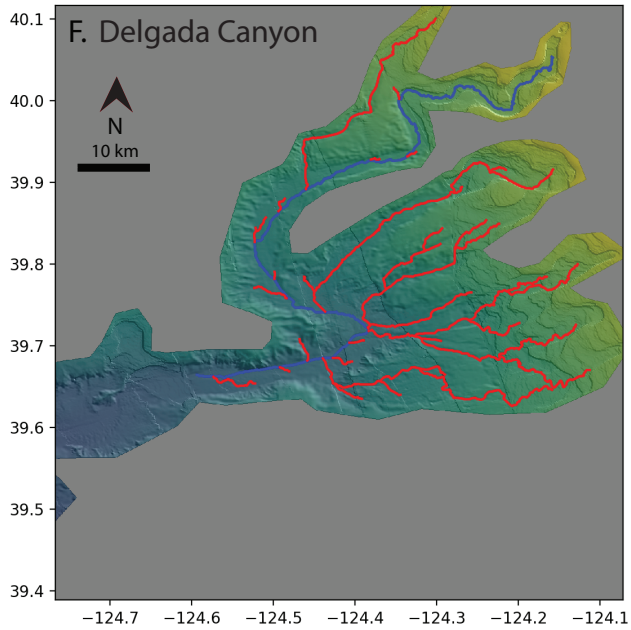

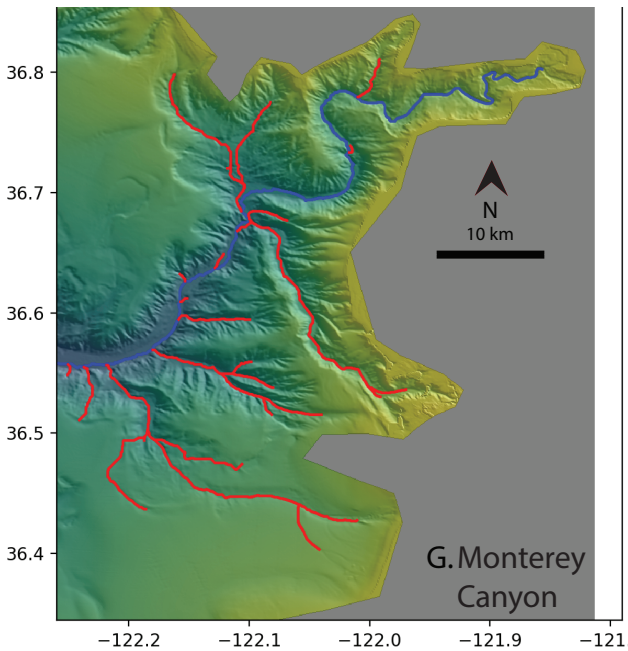

DOBBS FIGURE S2

TABLE S1. RESULTS FROM CHI ANALYSES

SUBAERIAL

Name	Location		Type	Area	θ_{ms}	R^2	θ_{tr}	R^2	$^{ms}k_s$	R^2	$^{tr}k_s$	R^2
	Latitude (°)	Longitude (°)		(km^2)								
Chappapeela creek	30.662	-90.636	Alluvial	7.1E+02	0.17	1.00	0.34	0.97	5.83	0.97	3.77	0.96
Amite River	30.703	-90.850	Alluvial	3.2E+03	0.18	1.00	0.29	0.98	7.22	0.94	4.83	0.96
Comite River	30.688	-91.068	Alluvial	5.5E+02	0.20	1.00	0.38	0.98	5.03	0.97	3.69	0.97
Choctawhatchee River	30.948	-85.844	Alluvial	7.8E+03	0.43	0.99	0.34	0.89	5.83	0.99	4.83	0.96
Pataula Creek	31.728	-85.086	Alluvial	1.6E+03	0.46	0.99	0.37	0.97	4.70	0.99	4.88	0.98
Little Cornie Bayou	32.718	-92.541	Alluvial	6.4E+02	0.46	1.00	0.32	0.97	3.42	1.00	3.65	0.97
Bayou D'Arbonne	32.732	-92.517	Alluvial	3.0E+03	0.40	0.98	0.41	0.93	3.62	0.97	3.85	0.99
Cornie Bayou	32.885	-92.610	Alluvial	1.8E+03	0.44	0.99	0.25	0.95	3.48	0.99	3.06	0.97
Bad Axe River	43.522	-91.205	Alluvial	7.9E+02	0.75	0.97	0.76	0.92	10.92	0.94	14.39	0.98
Ribeira de Lavre	38.816	-8.662	Alluvial	9.7E+02	0.48	0.99	0.61	0.92	8.76	0.99	9.35	0.99
Qoqek 1	43.981	85.441	Bedrock	2.0E+03	0.33	0.99	0.53	0.91	262.09	0.98	187.75	0.96
Qoqek 2	44.023	84.975	Bedrock	1.6E+03	0.45	0.99	0.53	0.89	181.35	0.99	162.10	0.95
Big Creek	36.859	-119.282	Bedrock	8.0E+03	0.55	0.96	0.27	0.82	199.55	0.95	233.81	0.77
North Fork Feather River	39.625	-121.496	Bedrock	7.2E+03	0.28	0.94	0.50	0.46	103.99	0.92	77.06	0.69
Butte Creek	39.706	-121.772	Bedrock	7.8E+01	0.46	0.95	0.51	0.94	100.50	0.95	69.47	0.94
Qoqek 3	43.877	86.239	Bedrock	8.1E+02	0.20	0.98	0.52	0.89	202.78	0.94	184.63	0.96
South Santiam River	44.413	-122.680	Bedrock	2.7E+03	0.69	0.98	0.61	0.88	50.50	0.95	55.89	0.98
Baluarte River	23.130	-105.682	Bedrock	4.8E+03	0.67	0.95	0.48	0.80	130.88	0.89	147.50	0.95
Tamazula 1	24.699	-106.555	Bedrock	1.5E+04	0.48	0.96	0.43	0.59	147.73	0.96	141.47	0.80
Rio Piaxtla	23.970	-106.264	Bedrock	4.8E+03	0.53	0.89	0.44	0.54	134.94	0.88	155.59	0.55
Tamazula 2	24.636	-106.386	Bedrock	8.6E+03	0.40	0.97	0.30	0.45	158.93	0.96	130.61	0.77
San Ignacio	24.116	-106.341	Bedrock	1.7E+03	0.56	0.94	0.49	0.77	147.33	0.93	174.57	0.88
North Santiam River	44.787	-122.805	Bedrock	2.8E+03	0.55	0.99	0.78	0.81	82.00	0.98	65.31	0.96
	AVERAGE			**3.5E+03**	**0.44**	**0.97**	**0.46**	**0.84**	**85.28**	**0.96**	**80.09**	**0.91**

SUBMARINE

Name	Latitude (°)	Longitude (°)	Type	Area (km^2)	θ_{ms}	R^2	θ_{tr}	R^2	$^{ms}k_s$	R^2	$^{tr}k_s$	R^2
Perth Canyon	-31.776	114.398	Shelf indenting	2.1E+03	0.15	0.98	-0.27	0.85	3.03	0.96	3.30	0.86
São Vicente Canyon	36.308	-9.925	Shelf indenting	2.3E+03	0.24	1.00	0.11	0.89	3.70	1.00	3.46	0.91
Setúbal Canyon	38.109	-9.903	Shelf indenting	1.5E+03	0.10	1.00	0.30	0.78	3.50	0.99	3.81	0.93
Cap Breton Canyon	44.174	-3.597	Shelf indenting	7.2E+03	0.23	1.00	0.17	0.72	1.74	1.00	7.21	0.91
Portimão Canyon	36.414	-8.571	Shelf indenting	9.6E+02	0.32	0.98	0.15	0.92	3.70	0.98	3.08	0.97
Delgada Canyon	39.664	-124.594	Shelf indenting	2.7E+03	0.21	1.00	0.11	0.92	2.04	1.00	2.69	0.98
Noyo Canyon	39.371	-124.616	Shelf indenting	1.2E+03	0.15	0.99	0.61	0.70	2.93	0.99	3.12	0.93
Monterey Canyon	36.344	-122.918	Shelf indenting	1.8E+03	0.17	0.99	0.02	0.88	3.02	0.98	5.61	0.81
Lacaze-Duthiers Canyon	42.296	4.105	Shelf indenting	3.3E+03	0.43	1.00	0.18	0.80	1.60	0.98	2.83	0.73
Petit Rhône Canyon	42.525	4.781	Shelf indenting	9.9E+02	0.48	0.99	0.47	0.91	1.94	0.97	4.54	0.98
Marseille Canyon	42.835	5.306	Shelf indenting	4.6E+02	0.41	0.97	0.31	0.95	3.99	0.96	4.63	0.86
Sète Canyon	42.519	4.257	Shelf indenting	6.5E+02	0.15	1.00	0.38	0.92	3.40	0.98	4.96	0.97
Nazaré Canyon	39.581	-10.221	Shelf indenting	3.0E+03	0.16	0.98	0.12	0.80	3.69	0.98	8.79	0.82
Partington Canyon	36.023	-122.349	Shelf indenting	9.8E+02	-0.32	0.98	0.14	0.56	2.72	0.86	3.42	0.99
Mill Creek Canyon	35.923	-122.126	Shelf indenting	1.1E+03	0.15	1.00	0.38	0.92	2.09	0.99	1.58	0.97
Sables d'Olonne Canyon	46.030	-4.559	Slope bound	9.9E+02	0.03	0.99	-0.32	0.94	7.74	0.98	8.57	0.77
Porcupine Canyon	50.153	-13.237	Slope bound	7.9E+03	0.43	0.99	0.50	0.95	1.17	0.96	1.65	0.86
Whittard Canyon	47.943	-10.207	Slope bound	2.2E+04	0.51	0.97	0.35	0.83	2.68	0.92	5.94	0.91
Biscay 1	47.023	-6.740	Slope bound	1.8E+03	0.83	0.96	0.49	0.91	3.49	0.82	9.01	0.94
Biscay 2	47.173	-6.946	Slope bound	1.3E+03	0.52	0.95	0.21	0.89	6.99	0.92	9.78	0.90
Biscay 3	46.850	-6.134	Slope bound	1.8E+03	0.70	1.00	0.38	0.85	5.42	0.92	2.11	0.93
Ireland Trough 1	54.310	-12.518	Slope bound	1.1E+03	0.11	0.99	0.03	0.94	3.85	0.98	5.13	0.96
Ireland Trough 2	54.406	-12.107	Slope bound	5.7E+02	0.07	0.99	0.13	0.93	4.93	0.99	6.98	0.99
Ireland Trough 3	54.486	-11.895	Slope bound	1.3E+03	0.26	0.04	0.42	0.93	4.38	0.99	4.05	0.97
Dawson Canyon	42.680	-60.880	Slope bound	1.1E+03	0.54	1.00	-0.01	0.93	3.34	0.97	5.05	0.98
Nova Scotia 1	42.597	-60.698	Slope bound	2.3E+03	0.35	0.99	0.09	0.91	3.46	0.99	3.31	0.95
Bonnécamps Canyon	42.905	-60.197	Slope bound	2.1E+03	0.32	1.00	0.25	0.89	3.93	0.99	4.67	0.95
Nova Scotia 2	42.789	-60.440	Slope bound	1.4E+03	0.35	0.99	0.09	0.91	3.72	0.99	4.03	0.97
Verrill Canyon	42.576	-61.050	Slope bound	2.6E+03	0.26	1.00	0.07	0.93	4.32	1.00	3.89	0.95
	AVERAGE			**2.70E+03**	**0.29**	**0.96**	**0.20**	**0.87**	**3.53**	**0.97**	**4.73**	**0.92**